Wave Number Selection and Large-Scale-Flow Effects due to a Radial Ramp of the Spacing in Rayleigh-Bénard Convection

Kapil M. S. Bajaj, Nathalie Mukolobwiez, Nathan Currier, and Guenter Ahlers
Department of Physics and Quantum Institute, University of California, Santa Barbara, California 93106
(Received 23 July 1999)

We present experimental results for wave numbers q_s selected in a thin horizontal fluid layer heated from below. The cylindrical sample had an interior section of uniform spacing $d = d_0$ for radii $r < r_0$ ($\Gamma_0 \equiv r_0/d_0 = 43$) and a ramp $d(r)$ for $r > r_0$. For Rayleigh numbers $R_0 > R_c = 1708$ in the interior, straight or slightly curved rolls with an average $\langle q_s \rangle = \tilde{q}_c + \alpha\epsilon_0(\epsilon_0 \equiv R_0/R_c - 1)$ and $\tilde{q}_c < q_c = 3.117$ were selected, and q_s varied on two length scales approximately equal to Γ_0 and to four roll wavelengths. For $\epsilon \lesssim 0.03$ and $\epsilon \gtrsim 0.18$ the pattern repeatedly formed defects.

PACS numbers: 47.54.+r, 47.20.Bp, 47.20.Lz, 47.27.Te

Many spatially extended nonlinear nonequilibrium systems undergo a transition from a uniform state to a state with spatial variation (a "pattern") when a control parameter R exceeds a critical value R_c [1]. Convection in a thin, wide horizontal fluid layer confined between two parallel rigid plates and heated from below [Rayleigh-Bénard convection (RBC)] has long been a paradigm of pattern formation [2]. Here R is the Rayleigh number

$$R = \beta g d^3 \Delta T/\kappa\nu \tag{1}$$

with β the isobaric thermal expansion coefficient, κ the thermal diffusivity, and ν the kinematic viscosity. The acceleration of gravity is g, and d and ΔT are the thickness of and the temperature difference across the layer. When ΔT exceeds ΔT_c (corresponding to $R = R_c$), a pattern of convection rolls forms. For $\epsilon \equiv R/R_c - 1 = 0$ the only stable pattern is one with a unique wave number q_c; but for $\epsilon > 0$ a continuum of states spanning a finite band of wave numbers is stable. The width of that stable band depends on the Prandtl number $\sigma \equiv \nu/\kappa$. For our $\sigma = 0.87$ and a laterally infinite system, its boundaries are shown by the solid line in Fig. 1. At large q the boundary is the skewed-varicose (SV) instability [3] at $q_{\mathrm{SV}}(\epsilon)$. At small q and ϵ, the Eckhaus (E) and crossroll (CR) instabilities [3] occur very close to each other near $q_E(\epsilon)$.

One of the issues in pattern formation is how a given system selects a particular wave number out of the continuous band of stable states. This selection problem has been studied only for a small number of specific cases [1]. An interesting mechanism for wave-number adjustment occurs when there is a spatial variation (a "ramp") of the control parameter from $\epsilon = \epsilon_0 > 0$ in a uniform section to $\epsilon < 0$ [4–7]. For the idealized case where the ramp has a vanishing slope, one expects that the selected wave number q_s at the point where $\epsilon = 0$ is equal to $q_c = 3.117$ [8]. This is predicted to be sufficient to fix q_s everywhere along the ramp and in the homogeneous interior and to lead to a time independent pattern near onset. For small ϵ_0, q_s in the interior is expected to be given by

$$q_s = \tilde{q}_c + \alpha\epsilon_0 \tag{2}$$

with $\tilde{q}_c = q_c$ and α dependent on the ramp and σ [5].

In the physical system the ramp angle is finite. Even for $R < R_c$ this usually leads to a large-scale flow (LSF), with a characteristic length scale much larger than a roll wavelength, which interacts with and modifies the roll structure above R_c. The interaction between LSF and the rolls is a broadly important issue in pattern formation at modest and small σ [9–13] because roll curvature also induces LSF which in turn reacts back on the roll pattern and modifies it. In patterns like the one in Fig. 2d, for instance, this leads to an emission of traveling waves by the wall foci, to the compression of rolls in the pattern interior beyond the SV instability, to repeated defect formation, and usually to chaotic time dependence. Since LSF and the rolls have complicated structures and are intimately coupled, it is difficult to study quantitatively the effect of one upon the other. The ramp offers a well posed situation where the LSF is "externally" generated and (at sufficiently small ϵ) independent of the roll pattern, and where a more detailed understanding of its interaction with the rolls should thus be possible.

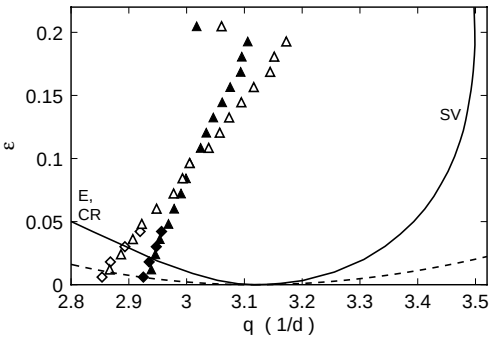

FIG. 1. Range of stable wave numbers for $\sigma = 0.87$. Solid line: Eckhaus (E), cross roll (CR), and skewed-varicose (SV) stability boundaries. Dashed line: the neutral curve. Solid symbols: ramp-selected q_s from two experimental runs, averaged over the uniform cell interior ($r \leq r_0$). Open symbols: averages for $r \leq r_0/2$.

 0031-9007/99/83(25)/5282(4)$15.00

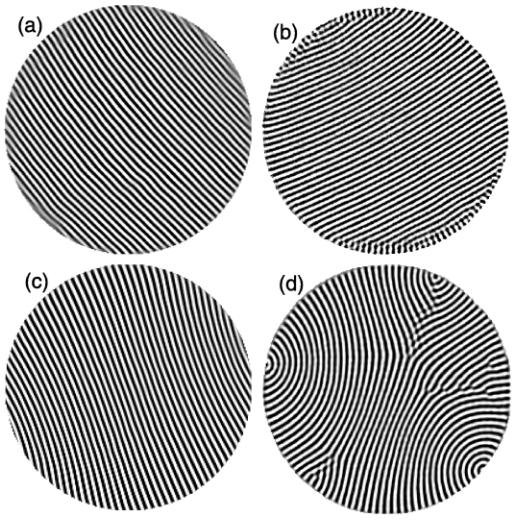

FIG. 2. Typical patterns from the present work for (a) $\epsilon_0 = 0.012$ and (c) $\epsilon_0 = 0.205$ and from Ref. [13] with rigid sidewalls and no ramp for $\sigma = 1.0$ with (b) $\Gamma = 43$, $\epsilon = 0.04$ and (d) $\Gamma = 40$, $\epsilon = 0.21$.

Here we present experimental results for a RBC cell with circular cross section, with a uniform central section of aspect ratio Γ_0, and with a *radial* ramp of d near the periphery. We found that $\tilde{q}_c < q_c$ (see Fig. 1). The pattern near onset repeatedly formed defects through the Eckhaus mechanism. This is consistent with $q_s < q_E$ for $\epsilon \lesssim 0.03$, but we note that the stability boundaries of the infinite system may be altered by the LSF. In the interior q_s was *not uniform* and the spatial variation of q_s was not rotationally symmetric even when roll curvature was virtually absent. It varied spatially on *two* length scales, one close to Γ_0 and the other about equal to 4λ [8]. The distribution of q_s changed as ϵ increased, q_s being small (large) in the cell interior at small (large) ϵ. For $\epsilon \gtrsim 0.18$, q_s locally exceeded the SV boundary of the infinite system and defects formed *via* the SV mechanism as seen before for rigid sidewalls [11,13]. We presume that these interesting and unexpected phenomena are a reflection of the interaction between the convection rolls and the LSF induced by the ramp, even though we cannot visualize the LSF directly.

Our apparatus was described elsewhere [14]. The fluid was SF_6 at a pressure of 20.04 bars with $\sigma = 0.87$. The sapphire top plate was at 37.50 °C. The bottom plate was diamond-machined aluminum [15]. Its central section of radius $r_0 = 3.18$ cm was optically flat and provided a section with a spacing $d_0 = 746 \pm 6$ μm uniform within 1 μm, corresponding to $\Gamma_0 \equiv r_0/d_0 = 42.6$. We estimated $\Delta T_c = 0.85 \pm 0.02$ °C from Eq. (1). The vertical thermal diffusion time $t_v = d_0^2/\kappa$ was 4.12 sec. Over the radius range $r_0 < r < r_1 = 4.44$ cm the bottom plate had a profile which yielded

$$\frac{d}{d_0} = 1 - \delta\left[1 - \cos\left(\frac{(r - r_0)\pi}{r_1 - r_0}\right)\right] \qquad (3)$$

with $\delta = 0.036$. Since $R \propto d^3$, $R/R_0 \propto (d/d_0)^3$. A paper sidewall was located immediately beyond r_1 but played no role since the pattern never reached it. We used shadowgraph visualization [14] for $0 < r \lesssim r_0$. For larger r the bottom-plate profile deflected the shadowgraph beam and no image was formed. The distance Δx between pixels was 211.7 $\pm$ 1 μm. Overall systematic errors of $\Delta x/d_0$, and thus of q, were no larger than 1.5% corresponding to $\delta q \simeq \pm 0.045$. In a typical run, we equilibrated the bottom-plate temperature for 2 h ($1750 t_v$) at a given ϵ and took 128 images at intervals of 1 min ($15 t_v$). In the interior we found $\Delta T_c = 0.830 \pm 0.001$ °C from the shadowgraph signal [16].

Figures 2a and 2c show the patterns which formed in two different experimental runs for $\epsilon = 0.012$ and 0.205, respectively. Within a given run the roll orientation changed very little with time, but from one run to another different orientations occurred. Whereas the rolls were nearly straight for $\epsilon = 0.012$, there was slight curvature for larger ϵ. For comparison we show in Figs. 2b and 2d patterns at similar ϵ from Ref. [13]. These were obtained in cells without ramps and with rigid sidewalls. The cross rolls which occurred without the ramp and at small ϵ near the sidewall (Fig. 2b) were absent in the ramped case (Fig. 2a). Likewise, at larger ϵ the wall foci, strong roll curvature, and domain-wall defects in the interior (Fig. 2d) did not occur in the presence of the ramp (Fig. 2c). Two factors which contribute to the difference come to mind. First, the ramp allows the roll amplitude to diminish gradually in the radially outward direction, and thus the tendency for the roll axes to terminate orthogonally to a sidewall is greatly reduced or eliminated. Second, LSF driven by roll curvature is diminished by dissipation in the ramped region [17]. On the other hand, LSF induced by the ramp itself can interact with the pattern and lead to the interesting effects which are central to this paper.

Mean pattern wave numbers obtained from Fourier analysis [18] of two separate runs are shown in Fig. 1. The solid symbols are for the entire uniform cell section with $r < r_0$ and the open ones were derived from the smaller region $r < r_0/2$. The data show that the azimuthally averaged q_s was larger (smaller) near the periphery than near the center when ϵ was small (large). At the largest ϵ, defect formation due to the SV instability occurred and thus the average q_s was shifted to smaller values.

To study the inhomogeneity of q_s, we determined the *local* q_s as a function of position in real space [19,20] using the methods of Ref. [20]. The results are shown in Fig. 3. The roll-axis orientation was from the upper left to the lower right. At small ϵ (Figs. 3a and 3b) q_s was relatively small in a band which extended through the cell interior parallel to the roll axes. Within this band, there was additional structure on a length scale of approximately 4λ [8,21]. As ϵ increased, the distribution

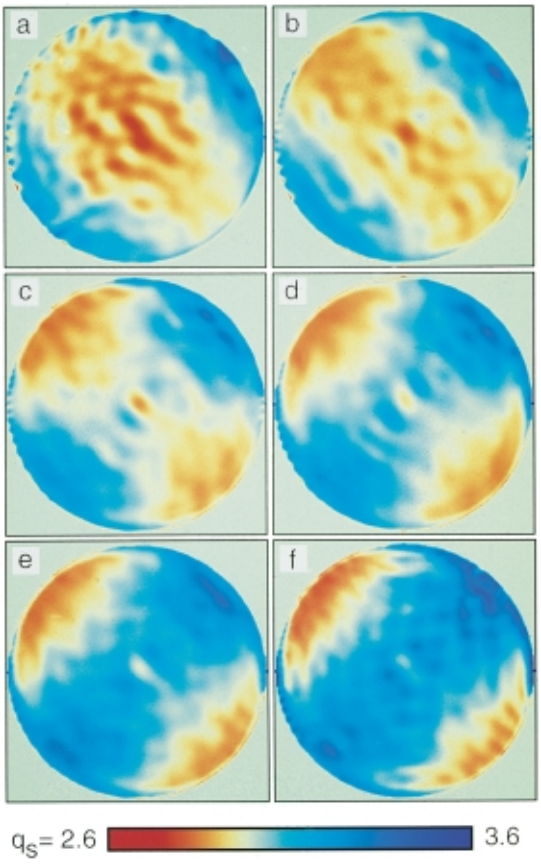

FIG. 3 (color). False-color representation of the local wave numbers q_s, each averaged over 128 images, for ϵ = (a) 0.012, (b) 0.048, (c) 0.084, (d) 0.120, (e) 0.157, and (f) 0.193.

of q_s evolved so that for $\epsilon \gtrsim 0.1$ the larger q_s occurred in a band which extended through the cell interior in a direction perpendicular to the roll axes. Again there was some structure with an intermediate length scale of about 4λ. The q_s variation at large ϵ was qualitatively different from what was found without ramps [11,13]. With rigid sidewalls and no ramp (see Fig. 2), the largest q_s occurred in the cell center, while in the ramped case it was found near the periphery.

For a better comparison between the patterns with ramps and with rigid sidewalls, we show in Fig. 4 the local q_s for the patterns of Figs. 2a and 2b, superimposed on the actual rolls. It is clear that the ramps yield a much stronger q_s variation than the rigid sidewalls.

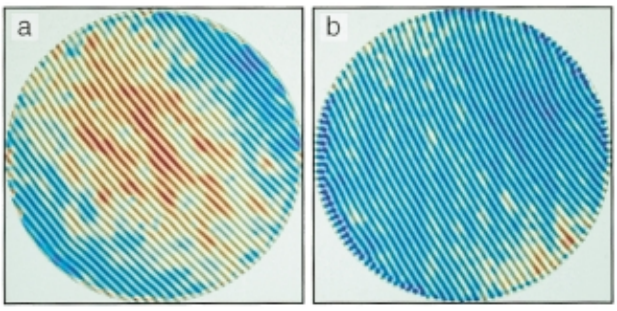

FIG. 4 (color). Patterns of Figs. 2a and 2b (rotated by $-90°$), superimposed on the local wave number q_s in false color.

The defect dynamics in the two time dependent regimes are illustrated in Fig. 5. Figures 5a and 5b show the dynamics at small ϵ in the Eckhaus-unstable regime [22]. Surprisingly, a defect pair formed near the periphery where the local q_s is relatively large (see Fig. 3a). One of the defects glided into the ramp and disappeared soon after its birth; the other glided into the cell center as seen in Fig. 5b. The solid (dashed) double-headed arrows are drawn parallel (perpendicular) to the unperturbed roll axes and reveal that the defect motion was indeed almost perfectly in the direction of the local wave vector, i.e., a glide motion without a significant climb component. After nearly reaching the cell center (not shown), this defect changed direction and climbed toward the lower-right periphery.

At large ϵ (Figs. 5c and 5d) a defect pair often is born near the cell center where q_s is somewhat smaller than near the periphery (see Fig. 3f). Again the solid arrow in the figure is parallel to the unperturbed roll axis, but the dashed arrow connects the defect pair. It makes the characteristic SV angle very close to $\pi/2 + \Theta_{\mathrm{SV}}$ ($\Theta_{\mathrm{SV}} = \pm 0.77$ rad) with the solid one. Events with both positive and negative Θ_{SV} were observed, and the defect pair sometimes formed closer to the periphery rather than in the cell center. After traveling some distance in the SV direction, the SV defects also changed direction and climbed to the periphery.

We are grateful to Werner Pesch for the use of his program to calculate $q_E(\epsilon)$, $q_{\mathrm{SV}}(\epsilon)$, and Θ_{SV}, and to Eberhard Bodenschatz, Fritz Busse, and Werner Pesch for

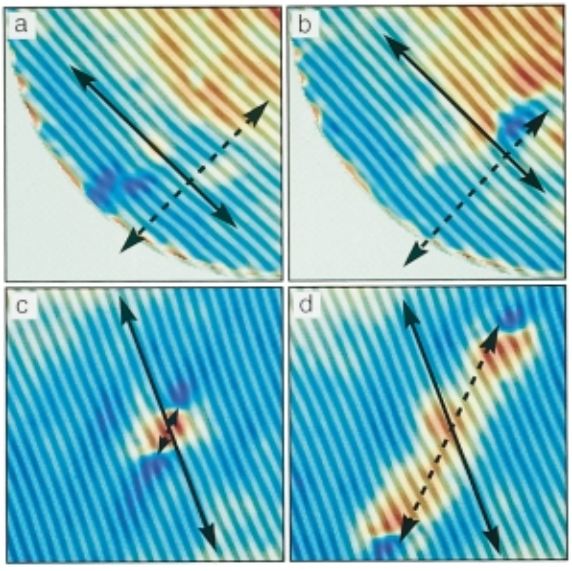

FIG. 5 (color). Defect-containing rolls, superimposed on the local q_s in false color. (a),(b): $\epsilon = 0.018$, 25 min ($350t_v$) apart. (c),(d): $\epsilon = 0.205$, 1 min ($15t_v$) apart.

stimulating discussions. This work was supported by U.S. Department of Energy Grant No. DE-FG03-87ER13738 and by National Science Foundation Grant No. DMR94-19168.

[1] See, for instance, M. C. Cross and P. C. Hohenberg, Rev. Mod. Phys. **65**, 851 (1993).

[2] For a review of work on this system during the last decade, see E. Bodenschatz, W. Pesch, and G. Ahlers, Annu. Rev. Fluid Mech. (to be published).

[3] R. M. Clever and F. H. Busse, J. Fluid Mech. **65**, 625 (1974); F. H. Busse and R. M. Clever, J. Fluid Mech. **91**, 319 (1979).

[4] For a review of the influence of ramps on pattern formation, see A. V. Getling, *Rayleigh-Bénard Convection: Structures and Dynamics* (World Scientific, Singapore, 1998).

[5] P. M. Eagles, Proc. R. Soc. London A **371**, 359 (1980); L. Kramer, E. Ben-Jacob, H. Brand, and M. C. Cross, Phys. Rev. Lett. **49**, 1891 (1982); I. C. Walton, Stud. Appl. Math. **67**, 199 (1982); Q. J. Mech. Appl. Math. **35**, 33 (1982); J. Fluid Mech. **131**, 455 (1983); L. Kramer and H. Riecke, Z. Phys. B **59**, 245 (1985); J. C. Buell and I. Catton, J. Fluid Mech. **171**, 477 (1986).

[6] H. Riecke and H. G. Paap, Phys. Rev. Lett. **59**, 2570 (1987); H. G. Paap and H. Riecke, Phys. Fluids A **3**, 1519 (1991).

[7] Excellent agreement between experiment [D. S. Cannell, M. A. Dominguez-Lerma, and G. Ahlers, Phys. Rev. Lett. **50**, 1365 (1983); M. A. Dominguez-Lerma, D. S. Cannell, and G. Ahlers, Phys. Rev. A **34**, 4956 (1986); G. Ahlers, D. S. Cannell, M. A. Dominguez-Lerma, and R. Heinrichs, Physica (Amsterdam) **23D**, 202 (1986); L. Ning, G. Ahlers, and D. S. Cannell, Phys. Rev. Lett. **64**, 1235 (1990)] and theory [6] for wave-number selection by ramps in quasi-one-dimensional systems was found for Taylor-vortex flow. For RBC, different ramps at the two ends of a narrow channel [I. Rehberg, E. Bodenschatz, B. Winkler, and F. H. Busse, Phys. Rev. Lett. **59**, 282 (1987)] led to traveling convection rolls. Theoretically the RBC case was considered by several authors [5]. However, we do not know of calculations for quasi-two-dimensional RBC with a radial ramp in d and for σ near 0.87 with rigid no-slip boundary conditions corresponding to the present experiment.

[8] We express lengths in units of d so that $q = 2\pi/\lambda$, where $\lambda = \tilde{\lambda}/d$ with $\tilde{\lambda}$ a roll wavelength.

[9] E. Siggia and A. Zippelius, Phys. Rev. Lett. **47**, 835 (1981).

[10] V. Croquette, M. Mory, and F. Schosseler, J. Phys. (Paris) **43**, 293 (1983); A. Pocheau, V. Croquette, and P. Le Gal, Phys. Rev. Lett. **55**, 1094 (1985); V. Croquette, P. Le Gal, A. Pocheau, and R. Guglielmetti, Europhys. Lett. **1**, 393 (1986); A. Pocheau, V. Croquette, P. Le Gal, and C. Poitou, Europhys. Lett. **8**, 951 (1987).

[11] V. Croquette, Contemp. Phys. **30**, 153 (1989).

[12] F. Daviaud and A. Pocheau, Europhys. Lett. **9**, 7 (1989); A. Pocheau and F. Daviaud, Phys. Rev. E **55**, 353 (1997).

[13] Y. Hu, R. Ecke, and G. Ahlers, Phys. Rev. E **48**, 4399 (1993); Phys. Rev. Lett. **72**, 2191 (1994); Phys. Rev. E **51**, 3263 (1995).

[14] J. R. deBruyn, E. Bodenschatz, S. Morris, S. Trainoff, Y.-C. Hu, D. S. Cannell, and G. Ahlers, Rev. Sci. Instrum. **67**, 2043 (1996).

[15] The diamond machining was done by Laser Power Optics, 12777 High Bluff Drive, San Diego, CA 92130.

[16] For $\Delta T = \Delta T_c$, the parameter $\mathcal{P}$ [see F. Busse, J. Fluid Mech. **30**, 625 (1967)] which describes the extent of departures from the Boussinesq approximation was 0.10. Theoretically, for this case a hexagonal pattern is expected to be unstable for $\epsilon \geq \epsilon_b = 1.8 \times 10^{-4}$, and the pattern of the infinite homogeneous system should consist of parallel straight rolls over our range of ϵ. We did not find any hexagons.

[17] This is similar to the reduction of curvature and mean flow studied in Ref. [12].

[18] The mean q_s was determined by taking the first moment of the square of the modulus of the Fourier transform [see S. W. Morris, E. Bodenschatz, D. S. Cannell, and G. Ahlers, Phys. Rev. Lett. **71**, 2026 (1993)].

[19] M. S. Heutmaker and J. P. Gollub, Phys. Rev. A **35**, 242 (1987).

[20] D. A. Egolf, I. V. Melnikov, and E. Bodenschatz, Phys. Rev. Lett. **80**, 3228 (1998).

[21] Structures in q of a one-dimensional system on intermediate length scales were observed under quite different circumstances by J. Lega, B. Janiaud, S. Jucquois, and V. Croquette, Phys. Rev. A **45**, 5596 (1992). We do not know whether there is any relationship to the present work.

[22] Since defects are finite-amplitude nonlinear structures, their experimentally observed motion in the direction of the wave vector (and thus of the original infinitesimal Eckhaus perturbation) was not necessarily expected *a priori*. For the SV case it was seen before [see Figs. 17 and 18 of Y. Hu, R. E. Ecke, and G. Ahlers, Phys. Rev. E **55**, 6928 (1997)] that the perturbation and the defect motion make nearly the same angle Θ_{SV} with the wave vector. The situation is different for strongly curved rolls which occur in smaller-Γ cells (see Figs. 20 and 23 of Ref. [11]), where the defects initially moved orthogonal to the wave vector and in the direction opposing the wave-number gradient.